# Reconstruction of stop quark mass at the LHC

Diego Casadei and Rostislav Konoplich*
*Department of Physics, New York University,*
*4 Washington Place, New York, NY 10003*

Rashid Djilkibaev
*Institute for Nuclear Research, Moscow, Russia 117312*

(Dated: July 1, 2010)

The cascade mass reconstruction approach was applied to simulated production of the lightest stop quark at the LHC in the cascade decay $\tilde{g} \to \tilde{\mathrm{t}}_1\,\mathrm{t} \to \tilde{\chi}^0_2\,\mathrm{t}\,\mathrm{t} \to \tilde{\ell}_R\,\ell\,\mathrm{t}\,\mathrm{t} \to \tilde{\chi}^0_1\,\ell\,\ell\,\mathrm{t}\,\mathrm{t}$ with top quarks decaying into hadrons. The stop quark mass was reconstructed assuming that the masses of gluino, slepton and of the two lightest neutralinos were reconstructed in advance.

A data sample set for the SU3 model point containing 400k SUSY events was generated which corresponded to an integrated luminosity of about 20 fb$^{-1}$ at 14 TeV. These events were passed through the AcerDET detector simulator, which parametrized the response of a generic LHC detector. The mass of the $\tilde{t}_1$ was reconstructed with a precision of about 10%.

## I. INTRODUCTION

If supersymmetry exists at an energy scale of 1 TeV, the study of third generation sleptons and squarks at the LHC is of a special interest. Their masses can be very different from that of sparticles of the first and second generation, because of the effects of large Yukawa and soft couplings as can be seen from the renormalization group equations. Furthermore they can show large mixing in pairs $(\tilde{t}_L, \tilde{t}_R), (\tilde{b}_L, \tilde{b}_R)$ and $(\tilde{\tau}_L, \tilde{\tau}_R)$. A detailed discussion of possible SUSY effects at the LHC is given in [1].

In this paper we consider the mass reconstruction of the lightest stop quark $(\tilde{t}_1)$ in the cascade decay

$$\tilde{g} \to \tilde{\mathrm{t}}_1\,\mathrm{t} \to \tilde{\chi}^0_2\,\mathrm{t}\,\mathrm{t} \to \tilde{\ell}_R\,\ell\,\mathrm{t}\,\mathrm{t} \to \tilde{\chi}^0_1\,\ell\,\ell\,\mathrm{t}\,\mathrm{t} \qquad (1)$$

with the top quarks decaying into hadrons. The gluino decay chain (1) is represented in Fig. 1, in which all final state particles are explicitly shown. Here, the considered leptons are electrons and muons ($\ell = \mathrm{e}, \mu$). The lightest neutralino $\tilde{\chi}^0_1$ is invisible to the particle detector, whereas b quarks and light quarks (labeled as 'q' in Fig. 1) are observed as jets.

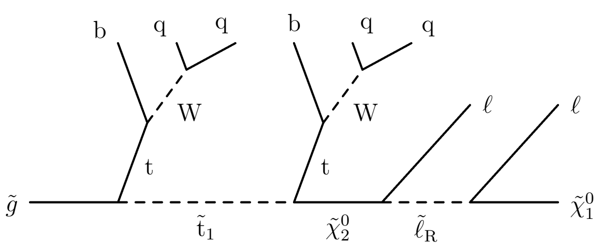


FIG. 1. A gluino cascade decay chain with a stop quark production.

Approaches to stop quark mass reconstruction in different decay chains and for different points in the MSSM parameter space are discussed in literature (for example in [2–7]). Recent limits from searches for stop quarks were published in [8].

The reconstruction of a SUSY event is complicated because of the escaping neutralinos and of the many complex and competing decay modes. At present, there are two different approaches to SUSY mass reconstruction. The *endpoint method*, which has been widely studied [2–4, 9–17], looks for kinematic endpoints of invariant mass distributions. The second method is the *mass relation approach* [18–21], based on the "mass relation equation" which relates the masses of the SUSY particles and the measured momenta of the detected particles. It was shown in [20] that the mass relation approach can be successfully used for integrated luminosities as low as a few fb$^{-1}$.

In this work, the mass relation approach of [20] is used for measuring the mass of the lightest stop quark $\tilde{\mathrm{t}}_1$, assuming about 20 fb$^{-1}$ of integrated luminosity in LHC proton-proton collisions at $\sqrt{s} = 14$ TeV, under the assumption that the masses of the gluino, slepton and of the two lightest neutralinos have been reconstructed in advance with 10–20% uncertainty. At such low integrated luminosity, the stop mass reconstruction is quite challenging because of a high level of SUSY background (sparticles created in decay chains different from that of Fig. 1) and Standard Model $\mathrm{t}\,\bar{\mathrm{t}}$ background.

In this paper, a particular example is chosen (the SU3 model; section II) to illustrate the method. First, an "event filter" is applied to suppress the background (section III), making use of a likelihood function built with the known uncertainties on jet and lepton measurements, constrained by the mass relation equation. Next, events which do not satisfy the kinematic limits derived from the chain (1) are discarded (section IV). Finally, a combinatorial mass reconstruction method (section V) is applied to find the best estimate of the stop mass from the maximization of a combined likelihood function, which

* Also at Manhattan College, Riverdale, New York, NY 10471

| Point | $m_0$ (GeV) | $m_{1/2}$ (GeV) | $A_0$ (GeV) | $\tan\beta$ | $\mu$ |
|---|---|---|---|---|---|
| SU3 | 100 | 300 | $-300$ | 6 | $> 0$ |

TABLE I. mSUGRA parameters for the SU3 point [1].

| Point | $m_{\tilde{g}}$ (GeV) | $m_{\tilde{t}_1}$ (GeV) | $m_{\tilde{\chi}_2^0}$ (GeV) | $m_{\tilde{\ell}_R}$ (GeV) | $m_{\tilde{\chi}_1^0}$ (GeV) | $\sigma$ (pb) |
|---|---|---|---|---|---|---|
| SU3 | 720.16 | 440.26 | 223.27 | 151.46 | 118.83 | 19 |

TABLE II. Theoretical masses and total production cross section $\sigma$ of SUSY particles at the SU3 point

depends on all five sparticle masses (gluino, stop, slepton and the two lightest neutralinos) and is constructed for each possible permutation of the final state particles.

## II. SIMULATION

The particular mSUGRA model chosen for this work is the bulk point SU3, one of the official benchmark points of the ATLAS collaboration [1], which is compatible with the recent precision WMAP data [22]. The values of the relevant mSUGRA parameters are given in Table I. For the SUSY particles in the cascade process (1), the theoretical masses and the production cross section have been found by ISAJET 7.74 [23] as reported in Table II.

The branching ratio for the gluino decay chain (1) at the SU3 point is

$$\tilde{g} \xrightarrow{25.2\%} \tilde{\mathrm{t}}_1 \xrightarrow{11.5\%} \tilde{\chi}_2^0 \xrightarrow{11.4\%} \tilde{\ell}_R \xrightarrow{100\%} \tilde{\chi}_1^0 \quad \Rightarrow \quad 0.33\%.$$

Monte Carlo simulations of SUSY production for the SU3 model point were performed with the HERWIG 6.510 event generator [24]. Later, the produced events were passed through the AcerDET detector simulation [25], which parametrized the response of a generic LHC detector (ATLAS and CMS detector descriptions can be found in [26] and [27]). The efficiency for b-jet reconstruction and labeling was set to 80%, whereas the calorimeter response to electrons and jets was

$$\mathrm{e}: \quad \frac{\sigma}{E} = \frac{0.12}{\sqrt{E/\mathrm{GeV}}} \,\oplus\, 0.005 \tag{2}$$

$$\mathrm{j}: \quad \frac{\sigma}{E} = \frac{0.5}{\sqrt{E/\mathrm{GeV}}} \,\oplus\, 0.03 \tag{3}$$

For muons, the same response function as for electrons has been used as first approximation.

A sample of 400k SUSY events (including signal and background processes) was generated. This approximately corresponds to 20 fb$^{-1}$ of integrated luminosity for the SUSY SU3 point production cross section of 19 pb at 14 TeV. The masses of $\tilde{g}$, $\tilde{\chi}_2^0$, $\tilde{\ell}_R$, $\tilde{\chi}_1^0$ listed in Table II were given as input and it was assumed that these masses had been already measured with about 10-20% uncertainty with the method explained in [20].

In order to isolate the chain (1) and to suppress the background, the following selection cuts were applied to the reconstructed quantities:

- exactly two isolated opposite-sign same-flavor (OSSF) leptons (either electrons or muons) with transverse momentum $p_\mathrm{T} > 20, 10$ GeV;
- two b-tagged jets with $p_\mathrm{T} > 50$ GeV;
- at least three jets with $p_\mathrm{T}$ larger than 150, 100, and 50 GeV
- at least nine jets with $p_\mathrm{T} > 10$ GeV (including b-tagged jets);
- no $\tau$-tagged jets;
- $M_\mathrm{eff} > 600$ GeV and $E_\mathrm{T}^\mathrm{miss} > 0.2 M_\mathrm{eff}$, where $M_\mathrm{eff}$ is the scalar sum of the missing transverse energy and the transverse momenta of the four hardest jets and $E_\mathrm{T}^\mathrm{miss}$ is the missing transverse energy;
- lepton invariant mass 50 GeV $< M_{\ell\ell} <$ 105 GeV.

A total of 24 signal and 191 background events are left after applying these cuts: the SUSY background to the signal process (1) is thus significant (the classification of events as signal and background is based on the knowledge of the simulated information).

As shown in [2], the SM processes are suppressed significantly by the above requirements. The SM dominant background surviving the hard cuts is $\mathrm{t}\,\bar{\mathrm{t}}$ production, where both W bosons decay leptonically producing a $\mathrm{b}\,\mathrm{b}\,l\,l$ state. Since the $\mathrm{t}\,\bar{\mathrm{t}}$ production cross section is about 833 pb, a 17M $\mathrm{t}\,\bar{\mathrm{t}}$ sample, corresponding to 20 fb$^{-1}$ of integrated luminosity, was generated with the HERWIG event generator. After applying the above selection cuts, only 21 $\mathrm{t}\,\bar{\mathrm{t}}$ background events survive.

Note that the requirement of high hadronic activity is important for the $\mathrm{t}\,\bar{\mathrm{t}}$ background suppression. If the cut on the total number of jets $N_\mathrm{jet} \geq 9$ is loosened to 7 jets, the number of $\mathrm{t}\,\bar{\mathrm{t}}$ events surviving the selection cuts increases to 115.

For every event, light jets (i.e. not tagged as b-jets) were combined in pairs whose invariant mass has been reconstructed. Only the independent pairs whose $M_\mathrm{inv}$ is in the range 60–100 GeV (W boson region) have been retained and events with less than two jet pairs have been rejected. The invariant mass distribution obtained with all combinations is shown in Fig. 2.

Next, all combinations of a $\mathrm{j}\,\mathrm{j}$ pair and a b-jet have been considered, retaining only those with $M_\mathrm{inv}$ =145–205 GeV, representing the acceptable W-b pairs in the top quark region (Fig. 3). After this step, from the initial 215 SUSY events (signal + background), a total of 834 $\mathrm{b}\,\mathrm{j}\,\mathrm{j}$ combinations were identified as candidates for a top quark decay $\mathrm{t} \to \mathrm{b}\,\mathrm{W} \to \mathrm{b}\,\mathrm{j}\,\mathrm{j}$, coming from 23 signal and 70 background events. Thus at this stage only one

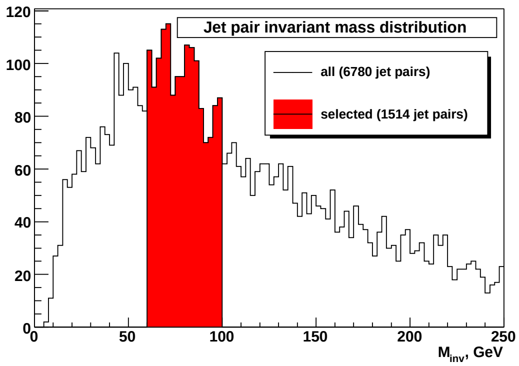


FIG. 2. Light jet pair invariant mass distribution. Only jj pairs with mass in the range 60–100 GeV have been retained in the analysis.

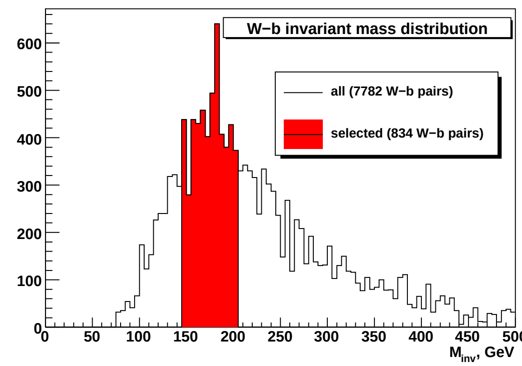


FIG. 3. W-b invariant mass distribution. W-b pairs are selected in the range from 145 GeV to 205 GeV.

signal event was lost. On the other hand, applying the same procedure to the 21 $t\bar{t}$ background events left only 3 events with 21 bjj combinations as candidates for a top quark decay.

Naively, one would think that this selection should let all $t\bar{t}$ background events survive, but it is clearly not the case. If a W-boson decays leptonically an invariant mass of light jets is not related with the W-boson mass. Also a parton showering leads to redistribution of energy and this means that the momenta of the b-quark and the W-boson are not sufficient to give the top invariant mass. The final result is that most $t\bar{t}$ events are dropped at this stage.

## III. BACKGROUND SUPPRESSION

To suppress the background before the last (combinatorial) step, an event filter is used which assumes that the masses of $\tilde{\chi}_2^0$, $\tilde{\ell}_R$, $\tilde{\chi}_1^0$ are known (Table II). The event filter maximizes, for each event, a likelihood function constrained by the mass relation equation, or equivalently minimizes the function:

$$\chi^2(m_{\tilde{g}}, m_{\tilde{b}}) = \sum_{i=1}^{4} \frac{(p_i^{\text{event}} - p_i^{\text{meas}})^2}{\sigma_i^2} + \lambda f(\vec{m}, \vec{p}) \qquad (4)$$

where the index $i$ runs over the two leptons and the two t-quarks, $p_i^{\text{meas}}$ and $\sigma_i$ are the reconstructed momentum and its uncertainty, and $p_i^{\text{event}}$ is the true momentum, which is varied to find the minimum (only uncertainties in jet and lepton energy measurements are taken into account). The parameter $\lambda$ is a Lagrange multiplier and $f(\vec{m}, \vec{p}) = 0$ is the mass relation.

The constraint $f(\vec{m}, \vec{p}) = 0$ is the key of the "mass relation approach": it relates the masses of the SUSY particles to the measured momenta of the final state particles in the chain (1) [18–20]. The mass relation constraint is obtained as a solution of a system of four-momentum constraints for each vertex containing SUSY particles in the decay chain (1). For example, for the gluino decay vertex one has $m_{\tilde{g}}^2 = (p_{\tilde{\chi}_1^0} + k_{l_1} + k_{l_2} + p_{t_1} + p_{t_2})^2$ where the right hand part is in terms of the four-momenta of the lightest supersymmetric particle (LSP), the detectable leptons, and the reconstructed top quarks. Similar relations can be obtained for each SUSY vertex in the process (1), which contains four vertices, hence one gets four kinematic equations that can be solved to find the four components of $p_{\tilde{\chi}_1^0}$ in terms of the SUSY masses and the momenta of the detectable and reconstructed particles. By substituting these components into the on-shell mass condition for the LSP, $m_{\tilde{\chi}_1^0}^2 = p_{\tilde{\chi}_1^0}^2$, the mass relation constraint includes all SUSY masses ($\vec{m}$) and the momenta ($\vec{p}$) of the detectable leptons and of the reconstructed t-quarks in the process (1). The explicit form of $f(\vec{m}, \vec{p}) = 0$ is given by [18–20].

Note that in the decay chain (1) the locations of each of the two t-quarks and of each of the two leptons are unknown. Here, it is assumed that the t-quark with higher energy originates from the gluino decay. In addition, we assumed that the leptons with higher $p_T$ originate from the $\tilde{\chi}_2$ decay. The momentum resolution for a t-quark is computed as $\sigma = \sigma_{\text{b-jet}} \oplus \sigma_{\text{jet 1}} \oplus \sigma_{\text{jet 2}}$, where all jets are assumed to have the resolution mentioned above (equation (3) in section II).

In the numerical minimization procedure by MC sampling, the gluino mass is left free to vary within $\pm 20\%$ from the value reported in Table II (a Gaussian sampling), and the stop mass is left free to vary uniformly in the range $480 \pm 120$ GeV because the stop mass is unknown at this step. The latter range has lower limit approximately related with the kinematic condition for a stop decay $m_{\tilde{t}_1} > m_{\tilde{\chi}_2^0} + m_t$ and is limited from above by the sbottom quark mass, which is about 600 GeV for the SU3 point.

For signal events, the event likelihood distribution has a maximum in the region of the ($\tilde{g}$, $\tilde{t}_1$) mass plane correlated with the true masses of $\tilde{g}$ and $\tilde{t}_1$. Hence, signal events should give a peak in the region of the true masses.

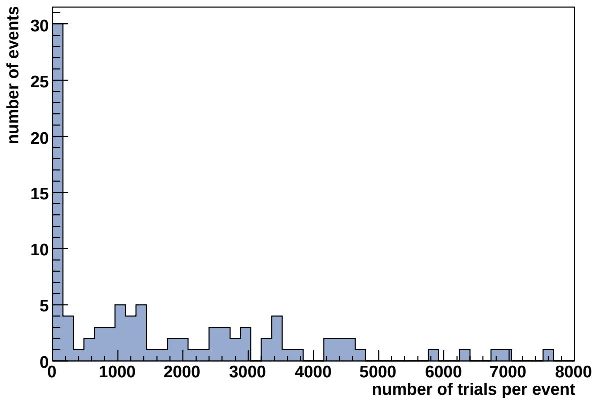


FIG. 4. The number of events versus the number of accepted trials per event with $\chi^2 < 10$. The total number of trials is $10^5$.

On the other hand, for background events there is no strong correlation between the likelihood maximum and the true masses of $\tilde{g}$ and $\tilde{t}_1$. Therefore, if we arbitrarily chose a point in the ($\tilde{g}$, $\tilde{t}_1$) mass plane in the range close to true masses, there is a very high probability that the value of $\chi^2$ found from equation (4) is smaller for a signal event than for a background one. For each event, $10^5$ points in the mass plane were generated in the range $720 \pm 144$ GeV for the gluino and $480 \pm 120$ GeV for the stop quark, and the $\chi^2$ was calculated. Results of event filter are presented in Fig. 4. This figure shows the number of events versus the number of trials per event in which $\chi^2 < 10$. Two groups of events can be seen: a group with the number of accepted trials close to zero and a group with more than a few hundred of accepted trials. The first group presents background events for which unlike for signal events a minimum of $\chi^2$ need not be in the considered mass range. Thus if $\chi^2 < 10$ in at least 300 trials per event, this event was considered as a signal candidate and was retained for the subsequent analysis.

Before the application of the event filter, we had 23 signal events, 70 SUSY background events and 3 Standard Model $\mathrm{t}\,\bar{\mathrm{t}}$ background events. After the application of the event filter, the SUSY background events were reduced approximately by a factor of 2 while a single signal event was lost: 22 signal events, 37 SUSY background events and 3 $\mathrm{t}\,\bar{\mathrm{t}}$ background events survived.

## IV. KINEMATIC LIMITS

It was shown [2–4, 9–17] that the endpoint method could be very useful in SUSY particle mass reconstruction for finding relations between the masses of the SUSY particles involved in a decay chain and to determine their masses. Such a method allows mass reconstruction without relying on a specific SUSY model. In particular, the endpoint method can be applied to a decay chain of the type

$$A \to b\,B \to b\,c\,C. \tag{5}$$

where particles $A$, $B$, $C$ are invisible but particles $b$ and $c$ are considered as visible (they can be either directly detected or indirectly reconstructed from the properties of final state particles).

In the literature, kinematic limits on the invariant mass distribution of $b\,c$ pairs in decay (5) over a variable $q^2 = (p_b + p_c)^2$ often are given for the case in which at least one of the visible particles is massless. However, in some cases both particles $b$ and $c$ can have a non-negligible mass. For example, this is the case when a gluino decays into a stop quark and top quark. These kinematic limits for the case of all massive particles in process (5) are given [28–30] by

$$q = \sqrt{(-R \pm \sqrt{R^2 - 4QS})/2Q} \tag{6}$$

with

$$Q = M_B^2 \tag{7}$$

$$\begin{aligned} R = {} & (m_b^2 - M_A^2 - M_B^2)\,(m_b^2 + m_c^2) + \\ & + (m_b^2 - M_A^2 + M_B^2)\,(M_B^2 - m_b^2 - M_C^2) \end{aligned} \tag{8}$$

$$\begin{aligned} S = {} & M_A^2\,(m_b^2 - m_c^2)^2 + \\ & + (M_A^2 - M_C^2)\ [m_b^2\,(M_B^2 - m_b^2 - M_C^2) + \\ & \qquad + m_c^2\,(M_A^2 + m_b^2 - M_B^2)] \end{aligned} \tag{9}$$

where the upper edge corresponds to the case when $b$ and $c$ particles are moving in opposite directions in the rest frame of particle $A$ and the lower edge corresponds to the case when $b$ and $c$ particles are moving in the same direction. A nonzero lower limit is a consequence of nonzero masses of the particles.

The kinematic limits from equation (6) for the process (1) are $q_{\min} = 375.1$ GeV and $q_{\max} = 496.8$ GeV for particles created on-shell. Because SUSY particles can also be created off mass shell, we have set a wider range. By choosing a cut at 525 GeV in $\mathrm{t}\,\bar{\mathrm{t}}$ invariant mass, the number of events remaining after the event filter selection is reduced to 21 signal events, 34 SUSY background events and 3 $\mathrm{t}\,\bar{\mathrm{t}}$ background events.

## V. STOP QUARK MASS RECONSTRUCTION

If all sparticle masses but the stop mass in the decay chain (1) were known, the mass relation equation would allow finding the stop mass directly. However, we assume that these masses are known at integrated luminosity of 20 $\mathrm{fb}^{-1}$ with an uncertainty of 10-20%. In order to take this into account, at the final step of the stop mass reconstruction we allow for all sparticle masses to vary in ranges defined by their uncertainties. Because in this case for each event there are five unknown masses, at least five events are required to reconstruct sparticle masses.

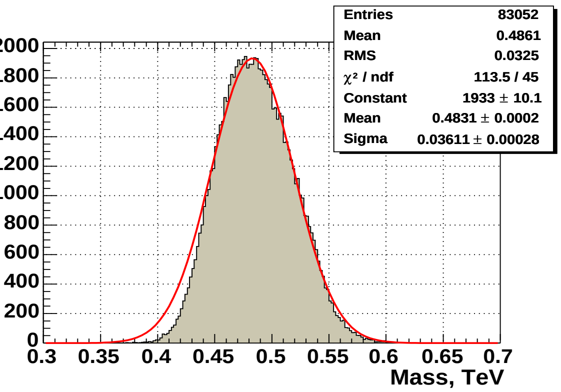


FIG. 5. Reconstructed stop mass distribution including SUSY background and SM $t\,\bar{t}$ background with integrated luminosity of 20 $\mathrm{fb}^{-1}$. The curve is the result of a Gaussian fit.

The combinatorial procedure of [20] is used for the final stop mass reconstruction, applied only to the events that pass the event filter. It is important to make the most effective cuts in advance, because such procedure is computationally very intensive due to combinatorics: all possible groupings of five events in the sample are considered.

For each set of five events, a combined likelihood function is built and maximized. For sparticle masses the combined likelihood function for the combination is defined as the product of the maximum likelihood functions for individual events. Finding a maximum of the combined likelihood function for the combination is the same as searching for a minimum of the function

$$\chi^2_{\mathrm{comb}}(\vec{m}) = \sum_{i=1}^{5} \min(\chi^2_{\mathrm{event}})_i . \qquad (10)$$

In Eq. (10), $\min(\chi^2_{\mathrm{event}})_i$ is a result of searching for a minimum of the $\chi^2_{\mathrm{event}}$ function for an individual event. For each of the five events in the combination, the $\min(\chi^2_{\mathrm{event}})$ is fitted with 9 parameters (four particle momenta and five SUSY masses).

The $\chi^2$ function for an individual event is defined by

$$\begin{aligned}\chi^2_{\mathrm{event}} &= \textstyle\sum_{i=1}^{4} \dfrac{(p_i^{\mathrm{event}} - p_i^{\mathrm{meas}})^2}{\sigma_i^2} + \\ &+ \textstyle\sum_{n=1}^{5} \dfrac{(m_n^{\mathrm{event}} - m_n)^2}{\sigma_n^2} + \lambda_1 f + \lambda_2 f^{\ell\ell}\end{aligned} \qquad (11)$$

where the variables with superscript “event” are those with respect to which one has to minimize.

The first term in equation (11) takes into account the deviations of the reconstructed momenta of the t-quarks, or the measured momenta of the leptons, from the true ones. The second term takes into account the intrinsic width of the SUSY particle masses, in the Gaussian approximation (instead of a Breit-Wigner distribution). The standard deviations corresponding to the mass widths are taken to be 15 GeV for the gluino, 2 GeV for the stop and 1 GeV for all light masses. The first two numbers are comparable with the theoretical widths for the heavy SUSY particles. The last number takes into account the fact that light SUSY particles are either quite narrow or stable. We note that the results of the mass reconstruction are not strongly sensitive to the actual values of sparticle widths. In equation (11) the mass relation and the $\ell\,\ell$ edge, which relates three light sparticle masses for chain (1), are included by means of the Lagrange multipliers $\lambda_1$ and $\lambda_2$. The $\ell\,\ell$ edge (103.1 GeV) can be obtained, for example, from Eq. (6) by plugging in the correspondent light sparticle masses and zero lepton masses.

The minimization is done numerically by means of MC samplings of the parameter space. The sampling is uniform for the stop mass, in the range: $480 \pm 120$ GeV. For the masses of $\tilde{g}$, $\tilde{\chi}_2^0$, $\tilde{\ell}_R$, $\tilde{\chi}_1^0$ a Gaussian sampling is done, with mean values as given in the Table II and standard deviations of 72, 20, 20, 20 GeV, which approximately corresponds to uncertainties of $10\%, 10\%, 15\%, 20\%$ in sparticle masses found in [20]. The MINUIT code [31] is used to search for the minimum of the $\chi^2_{\mathrm{comb}}$ function (10).

The reconstructed SUSY particle mass distribution, together with a Gaussian fit, is shown in Fig. 5. As can be seen in this figure, the reconstructed stop mass distribution is described approximately by a Gaussian with the mean value of 483 GeV and standard deviation 36 GeV.

The asymmetry of the stop mass distribution toward higher masses can be explained by the nearness of the kinematic edge for the stop decay $\tilde{t}_1 \rightarrow \tilde{\chi}_2^0 + t$ to the stop mass so that high masses are generated more often than lower values. This is not accounted for in the Monte Carlo sampling, for which we have uniformly generated the values of the stop mass.

In order to understand the role of background and of the simulated detector effects, the stop mass has been reconstructed using generator-level momenta without SUSY background and Standard Model $t\,\bar{t}$ background, and the result is shown in Fig. 6. In this case, as expected, the reconstructed stop mass is very close to the theoretical mass and the width of the distribution is smaller because of the absence of detector effects. It follows from comparison of Fig. 5 and Fig. 6 that the presence of background tends to shift the stop mass peak position to the region of higher masses.

## VI. CONCLUSION

We applied the cascade mass reconstruction approach developed in [20] for reconstructing the mass of the $3^{\mathrm{rd}}$ generation supersymmetric quark, assuming 14 TeV proton-proton collisions at the LHC with integrated luminosity of about 20 $\mathrm{fb}^{-1}$. At such relatively low integrated luminosity, the stop mass reconstruction is complicated

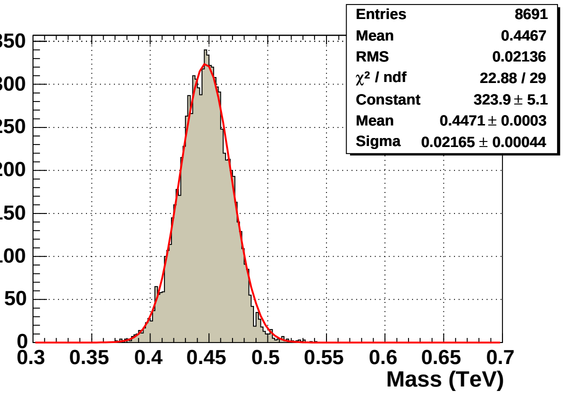


FIG. 6. Reconstructed stop mass distribution for true events without background with integrated luminosity of 20 $\mathrm{fb}^{-1}$. The curve is the result of a Gaussian fit.

because of a high level of SUSY and Standard Model $t\,\bar{t}$ backgrounds and of the low branching ratio for the gluino decay chain involving a stop quark. Our approach to the stop mass reconstruction is based on the consecutive use of an event filter and of a combinatorial mass reconstruction method.

In this work, we considered the stop mass reconstruction at the SU3 mSUGRA point and we obtained an estimate of the stop mass with a precision of about 10%. We expect that our approach should work for different MSSM parameters as well, provided that a decay chain containing at least four successive two-body decays and involving five SUSY particles has a sufficiently large branching ratio to be identified in a heavy background environment.

## ACKNOWLEDGMENTS

The authors thank M. Ibe, A. Mincer and P. Nemethy for interesting discussions and useful suggestions. This work has been supported by the National Science Foundation under grant PHY-0854724.


[1] The ATLAS Collaboration (G. Aad et.al.), arXiv:0901.0512 (2009).

[2] B.K. Gjelsten et al., ATLAS internal note ATL-PHYS-2004-007 (2004), published in The LHC/LC Study group (G. Weiglein et al.), arXiv:hep-ph/0410364.

[3] J. Hisano, K. Kawagoe, R. Kitano and M.M. Nojiri, Phys. Rev. **D66** (2002) 115004.

[4] J. Hisano, K. Kawagoe and M.M. Nojiri, Phys. Rev. **D68** (2003) 035007.

[5] I. Borjanovich, J. Krstic and D. Popovich, ATLAS internal note ATL-PHYS-CONF-2006-010, Geneva: CERN, 2006.

[6] S. Kraml and A.R. Raklev, AIP Conf. Proc. 903 (2007) 225.

[7] S.P. Mehdiabadi, CMS internal note CMS-CR-2006-010, Geneva: CERN, 2006.

[8] The CDF Collaboration (T. Aaltonen et al.), arXiv:hep-ex/0912.1308.

[9] H. Baer, K. Hagiwara and X. Tata, Phys. Rev. **D35** (1987) 1598;
H. Baer, D.D. Karatas and X. Tata, Phys. Rev. **D42** (1990) 2259;
H. Baer, C. Kao and X.Tata, Phys. Rev. **D48** (1993) 5175;
H. Baer, C. Chen, F. Paige and X. Tata, Phys. Rev. **D50** (1994) 4508.

[10] The CMS Collaboration (S. Abdullin et al.), J. Phys. **G28**(2002)469.

[11] I. Hinchliffe et al., Phys. Rev. **D55** (1997) 5520;
I. Hinchliffe and F.E. Paige, Phys. Rev. **D61** (2000) 095011;
H. Bachacou, I. Hinchliffe and F.E. Paige, Phys. Rev. **D62** (2000) 015009.

[12] B.C. Allanach, C.G. Lester, M.A. Parker and B.R. Webber, JHEP**0009** (2000) 004.

[13] B.K. Gjelsten, D.J. Miller and P. Osland, JHEP**12** (2004) 003.

[14] B.K. Gjelsten, D.J. Miller and P. Osland, JHEP**0506** (2005) 015.

[15] C.G. Lester, M.A. Parker and M.J. White, JHEP**0601** (2006) 080.

[16] A.J. Barr, B. Gripaios and C. Lester, JHEP**02** (2008) 014.

[17] A.J. Barr and C. Lester, arXiv:hep-ph/1004.2732.

[18] M.M. Nojiri, G. Polesello and D.R. Tovey, arXiv:hep-ph/0312317.

[19] K. Kawagoe, M.M. Nojiri and G. Polesello, Phys. Rev. **D71** (2005) 035008.

[20] R.M. Djilkibaev and R.V. Konoplich, JHEP **0808** (2008) 036.

[21] R.M. Djilkibaev and R.V. Konoplich, arXiv:hep-ph/0910.2448.

[22] D.N. Spergel et al., ApJS **170** (2007) 377.

[23] F.E. Paige, D. Protopopescu, H. Baer and X. Tata, arXiv:hep-ph/0312045.

[24] G. Marchesini et al., Comput. Phys. Commun. **67** (1992) 465;
G. Corcella et al., JHEP**0101** (2001) 010;
S. Moretti et al., JHEP**0204** (2002) 028.

[25] E. Richter-Was, arXiv:hep-ph/0207355.

[26] The ATLAS Collaboration (G. Aad et.al.), JINST **3** (2008) S08003.

[27] The CMS Collaboration (S. Chatrchyan et.al.), JINST **3** (2008) S08004.

[28] C.G. Lester, CERN-THESIS-2004-003, Geneva: CERN,2001.

[29] A. Bartl et al., Phys. Lett. **B679** (2009) 260.

[30] J. Di Bello, R. Konoplich, N. Lavini and T. St.Laurent, arXiv:hep-ph/1004.4819.

[31] F. James and M. Roos, Comput. Phys. Commun. **10** (1975) 343.